Performance Based Analysis of Watermist Protection System in a Conveyor Belt using CFD

Patricio Valdés Gacitúa[1], Miguel Ángel Pérez Arias[2]

[1]MAPA Fire engineering, Santiago, Chile, patricio.valdes@mapafire.com
[2]MAPA Fire engineering, Santiago, Chile, miguel.perez@mapafire.com

MAPA Fire Engineering
La Serena 138, La Florida
Santiago, Región Metropolitana, 8320000, Chile
e-mail: patricio.valdes@mapafire.com

ABSTRACT

[*Background*] Usually, sprinklers systems from prescriptive codes are used for the protection of conveyors belts in mining. However, due to an increasing environmental concern with the sprinkler´s water discharged, a demand for optional fire protection systems has arisen.
[*Objective*] The aim of this study was to investigate whether water mist fire protection systems could provide an equal level of protection, as compared to a regular sprinkler system.
[*Method*] A series of CFD simulations using FDS were conducted in accordance to the recommendations given in the FM-Global datasheet protection for conveyor belts, several variations of sprinkler system arrangement and commercially available water mist fire protection systems. The simulations were conducted representing the worst probable and credible fire scenario, which corresponds to a fire in the 130m section of the conveyor belt with 10° of slope. The HRR produced by the fire developed ranging up to 8 MW, considering the material of the conveyor belt and the fire propagation.
[*Results*] The CFD simulations revealed that the sprinklers systems controlled and extinguished the fire in fractions of minutes, as well as the watermist system. On the other hand, the watermist system requires much less water to control the fire and therefore, the amount of water discharged to the environment is much less than the sprinklers system.
[*Main conclusions and recommendations*] It is concluded that the protection of closed conveyor belt with a slope are viable with water mist fire protection systems, with the same performance than a sprinklers system but affecting much less the environment where the conveyor belt is placed.

Keywords: Flammable, liquids, rack, storage, sprinklers, FDS, NFPA 30, NFPA 13, Simulations, Fire, Full-scale test, CFD, thinners, paints, ethanol.

INTRODUCTION

Chilean mining company requires the installation of an active fire protection system in the mineral transport system, specifically in the conveyor belts over a pier that transport copper concentrate from the mining process to the transportation ships.

The mining company desires to fulfil the fire protection goals of; life safety, operational continuity and minimize the environmental impact of water protection system discharged, due to the conveyors belts are transporting copper concentrate over the water (sea). Thus, an eventually discharge from the fire protection system would contaminate the sea water.

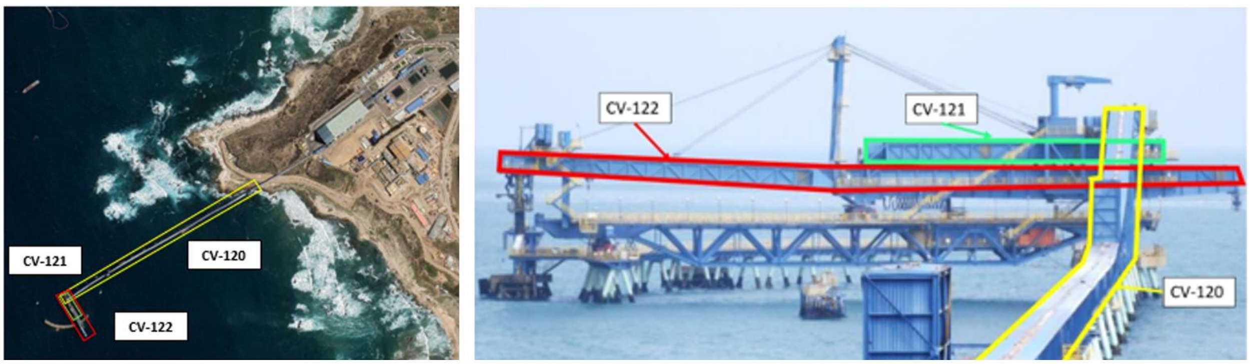

Figure 1: Left - Aerial view of the facilities/Right – POV facilities, starting at first conveyor belt.

To avoid sea water contamination, the company needs to contain the eventual water discharge from the fire protection system. A bigger water flow needed for fire control and extinguishment would need a bigger drainage and accumulation system installed in the structure of the conveyors belt above the sea. Therefore, under this requirement that a performance base analysis is developed to minimize the water drainage system and the potential contamination of the sea water.

METHODOLOGY

The general methodology to assess the present study is described in the Figure 2.

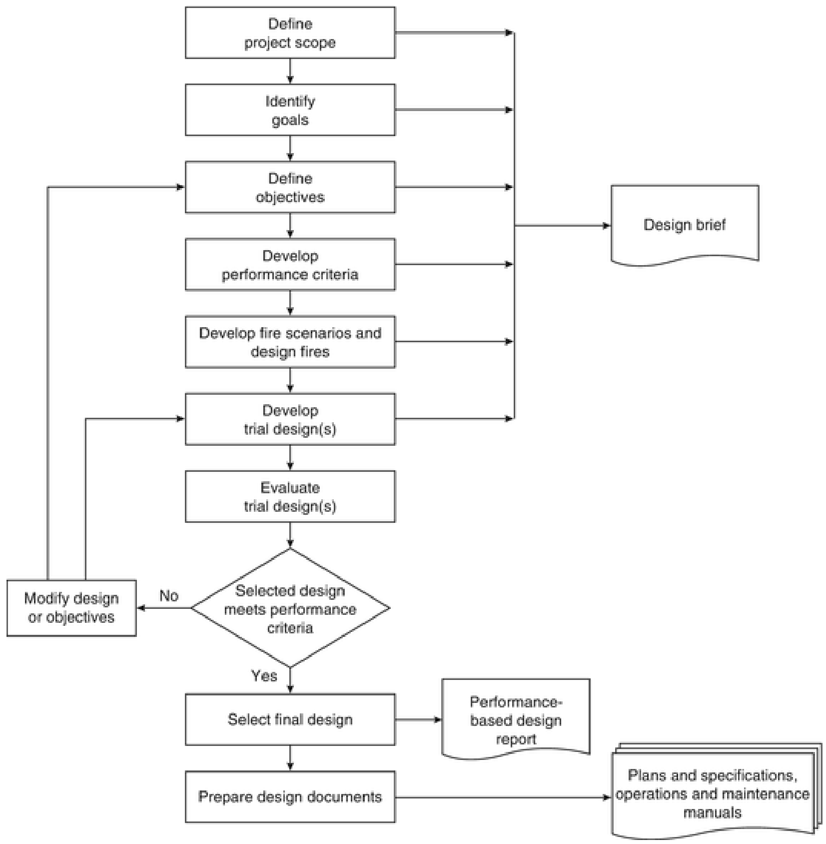

Figure 2: General methodology for PBD according SFPE Handbook [1]

Scope

The scope of the study corresponds to the conveyor belts indicated in the Figure 1.

Goals

The goals correspond to:

- Provide an environment reasonably safe from fire for occupants that's are not closely related to the initial development of the fire and improve the survival capacity of the occupants closely related to the initial development of the fire.
- Provide an environment for the protection of property and operational continuity in the event of a fire, considering the environmental protection requirements.

Objectives

1) Protection of the occupants: evaluate a fire protection system that protects the occupants who are not familiar with the initial development of the fire during the time necessary to evacuate. Allow occupants who are closely related to the fire to evacuate in sustainable conditions for life safety.
2) Operational continuity: Evaluate a fire protection system that minimizes the impact of fire in the facilities, considering the fire propagation, heat released rate, among others.
3) Minimize the water discharge: evaluate a fire protection system that allows compliance with objectives 1 and 2 before mentioned and that also fulfils the environmental requirements of minimize the water containment.

Performance Criteria

The performance criteria considered in the current analysis correspond to the following:

- Visibility.
- FED.
- FIH.
- Process Equipment Temperature.
- Fire spread and Combustion Control.
- Time to Control and Extinguish the Fire.
- Structural Stability.
- Thermal radiation.
- Water discharged.

For the present paper, the water discharged is the variable analyzed that allows to compare the performance of the different trial designs, due to that is expected that all the systems will control and extinguish the fire while fulfilling the rest of performance criteria.

Fire Scenarios

Along a conveyor belt there is available a large amount of combustible materials, including the conveyor belt itself, rollers, grease, and oil. The continuous distribution of combustible material along the drift of the conveyor and the longitudinal ventilation that aids in the spread of the flame will challenge any fire protection system and the fire safety of the facility. Fires on non-fire-resistant conveyor belts produce higher rates of heat released, a higher rate of fire growth and a faster rate of flame spread.

Therefore, the fire scenario analyzed considers that the fire starts in the area where the belt presents a greater slope, considering an average angle of 10° of inclination and 130m length (Figure 3).

The scenario also considers that the belt stops due to the activation of detection system and the auxiliary systems also stop when the detection system operates.

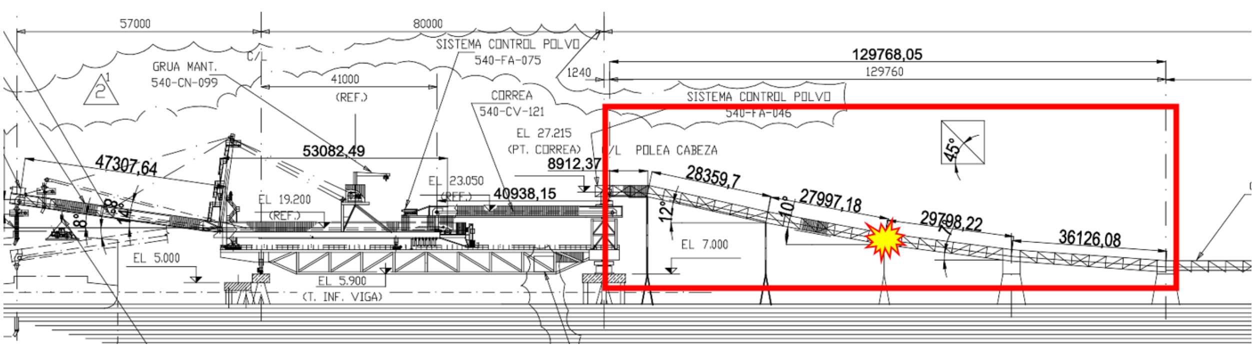

Figure 3: Fire localization

Trial Designs

Trial designs corresponds to the fire protection strategies that are intended to fulfil the project objectives. To be considered acceptable, the trial designs must fulfil the performance criteria when fire scenarios are analyzed.

Evaluation of Trial Designs

The evaluation of the trial designs is intendent to analyze, compare and review the results regarding if the performance criteria is fulfilled or not and if the objectives of the study are also fulfilled.

PERFORMANCE CRITERIA

The performance of the water-based test designs will be analyzed regarding the fire protection requirements by Factory Mutual in the Datasheet 7-11 Art. 2.3.3 (Table 1). Therefore, the water-based fire protection trial designs will be analyzed against Factory mutual design and therefore, against the expected operation (Table 2).

Table 1: FM Requirements summary

K Factor	8	US
Pressure	15	PSI
Flow per Sprinkler	31	gpm
Flow per 10 Sprinklers	310	gpm
	1171	lpm

Table 2: Real operation according to simulation

Opened Sprinklers	5	Un
Total Flow	155	gpm
	586	lpm
Average Activation Time	22.3	sec

FIRE SCENARIOS

To evaluate the fire performance of the system, two fire scenarios has been considered. The first one corresponds to a fire in the conveyor belt without considering the fire protection systems (existent condition). The second scenario contemplate the operation of the fire protection systems designed in the chapter "Mesh and Cell Size

For the initial grid resolution, the expression stated in the FDS User Guide has been considered. For simulations involving buoyant plumes, a measure of how well the flow field is resolved is given by the non-dimensional expression $\frac{D*}{\delta x}$, where D* is a characteristic fire diameter and δx is the nominal size of a mesh cell.

$$D^* = \left(\frac{Q}{\rho\ C\ T\ \sqrt{g}}\right)^{\frac{2}{5}} \qquad \text{Equation 5}$$

Where $\dot{Q}$ is heat release rate of the fire is, ρ is the air density at ambient temperature, C correspond to the air specific heat, T is the ambient temperature and g is the acceleration due to gravity. In a sensitivity analysis (Hill et al., 2007), sponsored by the U.S. Nuclear Regulatory Commission, the D * / Δx value ranges between 4 and 16.

As a cell size criterion, the following relationship of numerical intervals will be used, where 4 will correspond to a poor resolution without affecting the values of the results and 16 will correspond to the greatest resolution without demanding a high cost of computational resources.

$$4 < \frac{D^*}{\delta x} < 16 \qquad \text{Equation 6}$$

Thus, by applying the before mentioned criteria and considering the values shown in the Table 4 it is possible to obtain the flow resolution quality indicator values for the combustion zone, and the plume zone of the hot gases produced by the fire in the conveyor belt.

Table 4: Parameters considered.

Ambient Temperature	1.2	kg/m3
Cp Ambient Air	1	kJ/kg °K
Ambient Temperature	293	°K
Gravity Acceleration	9.81	m/s2

The mesh geometry will be built considering cubic cells with a symmetrical configuration. The entire computational domain will be divided into different meshes with different cell sizes, allowing to cover the computational domain without overusing cells.

The Figure 17 contains the meshing technique, where the conveyor belt zone contains the smallest cell in the domain and then the fire plume contains cells with a middle size. The biggest cell size is used in the lower part of the domain, where the fresh air inlet for the fire is located.

The sensitivity analysis for the cell size shown in the Figure 17 and according to the to the Equation 5 and Equation 6 is indicated in the Table 5 and Table 6, where and indicator of a great flow resolution is shown.

The 2 MW used as a prior HRR to assess the sensitivity analysis it has been developed by previous research [], where it is possible to find that the early stage of the fire in a similar conveyor belt develop a HRR of 2MW (Figure 16).

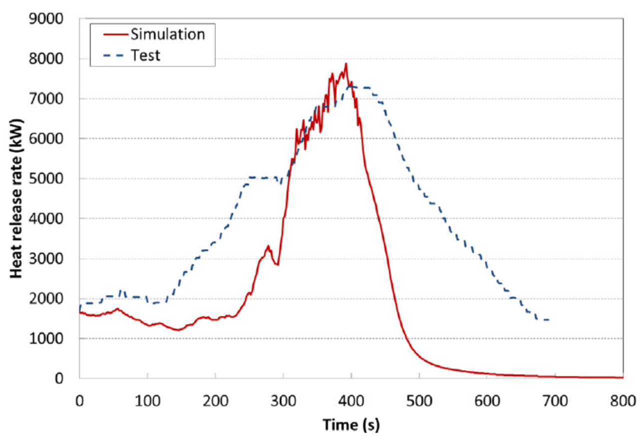

Figure 16: HRR Simulated and tested in a similar conveyor belt.

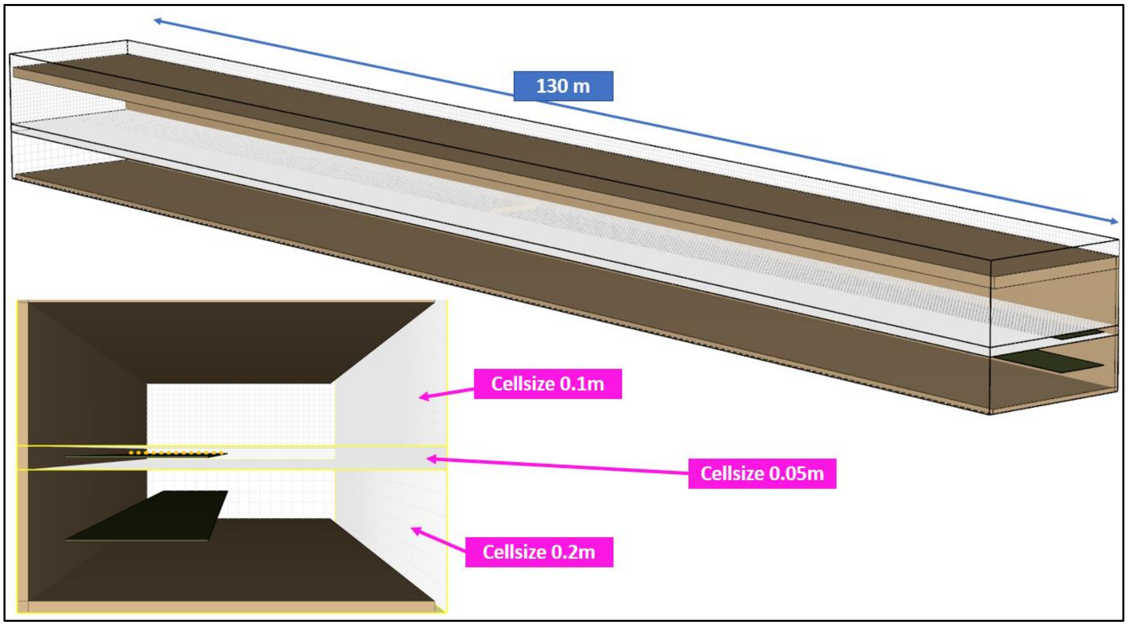

Figure 17: Meshing technique

Table 5: Cellsize Combustion Zone

Scenario	HRR		D*	Cellsize (m)	D*/Cellsize
Scenario 01	2000	kW	0.8041	0.05	16
Scenario 02-05-A	2000	kW	0.8041	0.05	16
Scenario 02-05-B	2000	kW	0.8041	0.05	16
Scenario 02-05-C	2000	kW	0.8041	0.05	16
Scenario 02-05-D	2000	kW	0.8041	0.05	16

Table 6: Cellsize Plume Zone

Scenario	HRR		D*	Cellsize (m)	D*/Cellsize
Scenario 01	2000	kW	0.8041	0.1	8
Scenario 02-05-A	2000	kW	0.8041	0.1	8
Scenario 02-05-B	2000	kW	0.8041	0.1	8
Scenario 02-05-C	2000	kW	0.8041	0.1	8
Scenario 02-05-D	2000	kW	0.8041	0.1	8

TRIAL DESIGNS” of the current document.

<u>Fire Scenario 01 - Conveyor Belt Fire</u>

Statistical Information

In a study of conveyor belt drive-in fires in underground coal mines, it was found that most fires were caused by friction in the belt drive along the length of the belt. Conveyor fires were found to be among the most common types of fires in the Australian mining industry after vehicle fires [2]. The most common causes of conveyor belt fires were:

- Faulty bearing causes the excess of grease to ignite.
- Defective roller or roller causing friction and igniting the roller.
- Friction between the conveyor and a roller or pulley.
- Metal in contact with the belt.

- Rocks stuck against a roller/conveyor causing friction.

The most common places for fire starting are the conveyor belt, belt roller, return roller, impact roller, idler pulley, bending pulley and head pulley.

Ignition

The ignition sources listed above justify a friction-caused fire for the fire scenario. Therefore, it is considered that one roller fails and causes friction, heating up the roller and igniting the belt (Figure 4). The diameter of the rollers is 133mm, which is considered as the fire ignition surface.

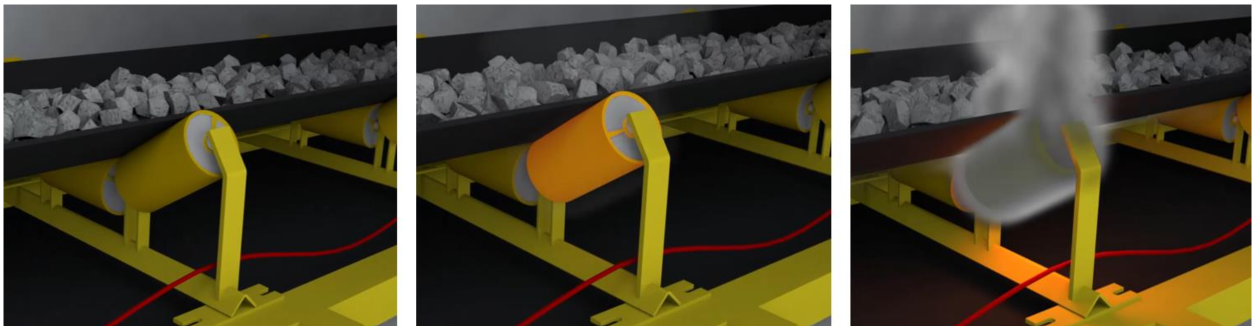

Figure 4: Typical sequence of ignition by heating up roller.

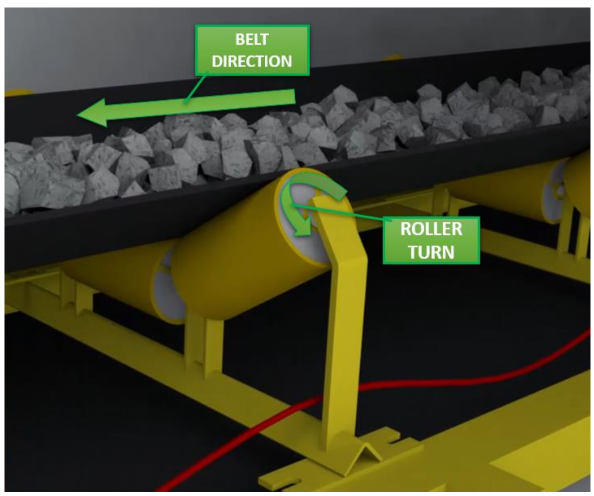

Figure 5: Normal Operation Conveyor Belt

When a roller stops due to some mechanical failure, there is a generation of heat due to friction between the belt and the idler. When this occurs, the roller increases temperature and heats up the zone of the belt in contact. After, the belt cools down due to the heat losses to the environment, according to the Figure 6.

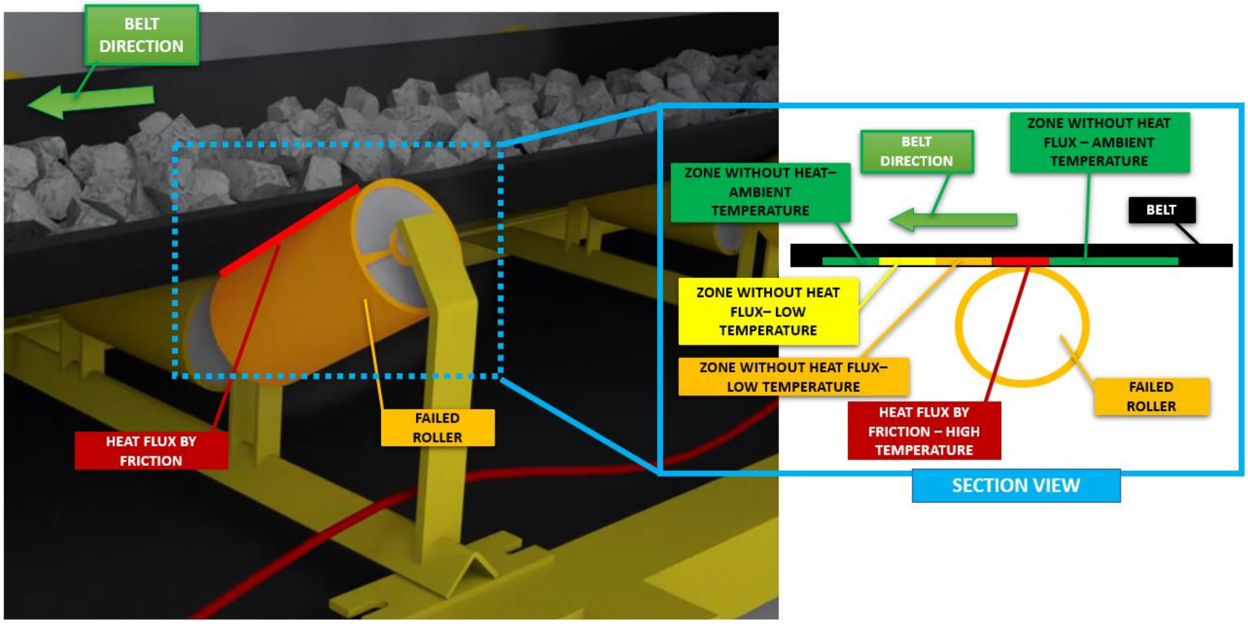

Figure 6: Failed roller with conveyor belt operating.

On the other hand, when the belt stops, the heat flux due to the friction is transmitted constantly to the belt in the same area, increasing the temperature of the material and contributing to the fire ignition. Thus, the belt will probably start to ignite when it stops and not when it is moving (Figure 7).

Therefore, the fire scenario considers that the conveyor belt will ignite when stops, developing a fire under no influence of the air velocity of the moving of the conveyor belt.

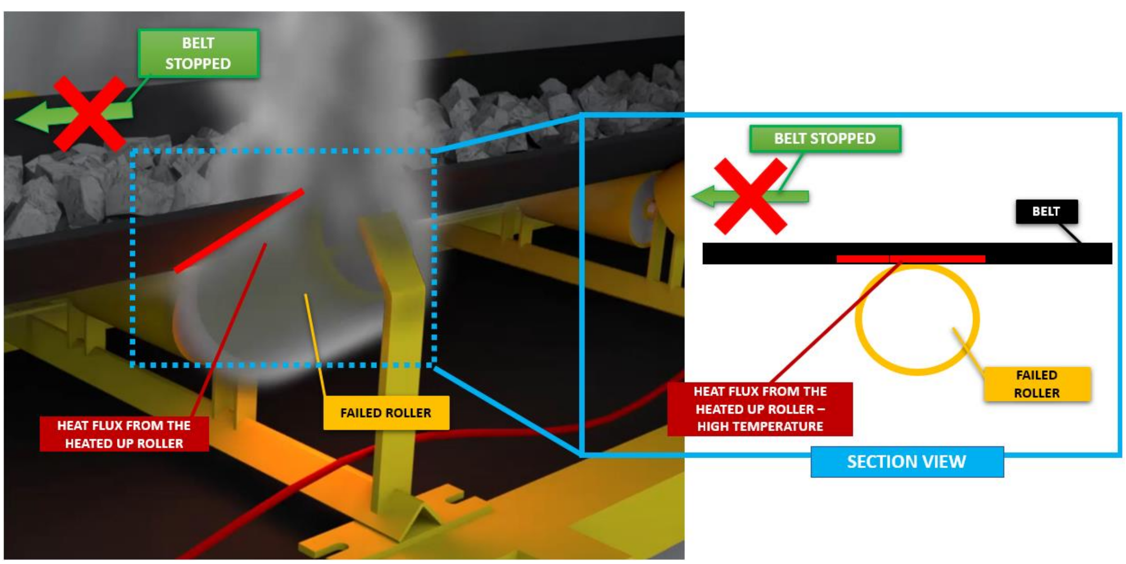

Figure 7: Failed roller with conveyor belt stopped.

Combustible

According to the manufacturer belt´s specification, the belt material corresponds to polyester and polyamide, which is designated as EP (Figure 8).

LTING:	SPECIFIED BY BECHTEL	SUPPLIER DATA (S)
MANUFACTURER		CONTI
BRAND NAME		
DESIGNATION/CODE		
TYPE:	X FABRIC STEEL CORD	FABRIC
BELT WIDTH	(SEE SHEET 1 OF 8)	1200,00 mm
TOTAL LENGTH:	INCLUDING SPLICE ALLOWANCE	1606 m
TAPED LENGTH:		1591 m
TENSION RATING:		2000 N/mm
MAX. OPER. TENSION:		208 N/mm
ULTIMATE TENSILE STRENGTH:	FABRIC BELT:	246 N/mm
	STEEL CORD BELT:	N/mm
BELT WEIGHT:		31,50 kg/m
FABRIC BELT:	TYPE OF FABRIC	EP
	NO. OF PLIES	5
	BREAKER ON FACE YES XX NO	
	BREAKER THICKNESS mm	mm
	TEMPERATURE RATING :	°C
	COEFF. OF THERMAL EXPANSION (HR):	
	FILL MATERIAL:	
	FRICTION RATING BETWEEN PLIES:	

Figure 8: Belt manufacturer specification

Due to the conveyor belt transport cooper concentrate, just the conveyor belt is considered as a burnable material. This supposition considers that the conveyor belt is empty and if the conveyed material is different than coal, it will be inert and it will act as a thermal sinker, decreasing the fire propagation. Therefore, the conveyor belt material properties are indicated in the Figure 9, while in the Figure 10 are specified the performance of the fire products considered for the conveyor belt material.

Property	Virgin material
Density (kg/m^3)	1300
Specific heat (kJ/kg/K)	1.3
Conductivity (W/m/K)	0.19
Heat of combustion (kJ/kg)	2.85×10^4
Heat of gasification (kJ/kg)	1500

Figure 9: Conveyor belt properties [3]

Material	ΔH_T (kJ/g)	y_{CO_2} (g/g)	y_{CO} (g/g)	y_{ch} (g/g)	y_S (g/g)	ΔH_{ch} (kJ/g)	ΔH_{con} (kJ/g)	ΔH_{rad} (kJ/g)
Synthetic materials–solids (abbreviations/names in the nomenclature)								
ABS[b]	–	–	–	–	0.105	30.0	–	–
POM	15.4	1.40	0.001	0.001	–	14.4	11.2	3.2
PMMA	25.2	2.12	0.010	0.001	0.022	24.2	16.6	7.6
PE	43.6	2.76	0.024	0.007	0.060	38.4	21.8	16.6
PP	43.4	2.79	0.024	0.006	0.059	38.6	22.6	0
PS	39.2	2.33	0.060	0.014	0.164	27.0	11.0	16.0

Figure 10: Fire products in well ventilated fires [4]

The conveyor belt contains multiple components; however, it is challenging characterize entirely the properties necessary for the fire modelling. Therefore, the conveyor belt will be contemplated as one burnable component, considering the lowest (thus the most critical) ignition temperature, which correspond to 250°C, according the Figure 11.

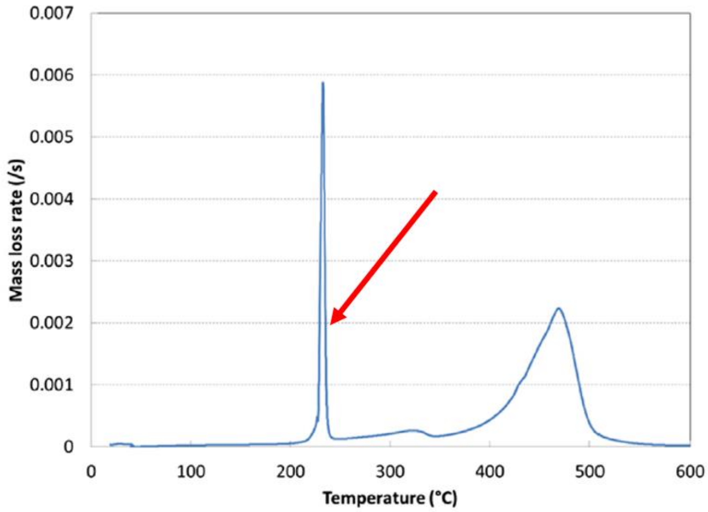

Figure 11: Ignition Temperature [5]

Fire Location and Geometry

Due to the length of the conveyor belt system covered by the scope of the investigation, the analysis has been implemented in a section of the conveyor belt, allowing to obtain precise and useful results without increasing the computational cost of the model.

Thus, the fire location is considered in the area where the conveyor belt presents the greatest slope, considering a total inclination of 10° over a 130m section (Figure 12). The fire location presents the worst-case scenario in terms of heat release rate, fire propagation and smoke production due to the sloped condition.

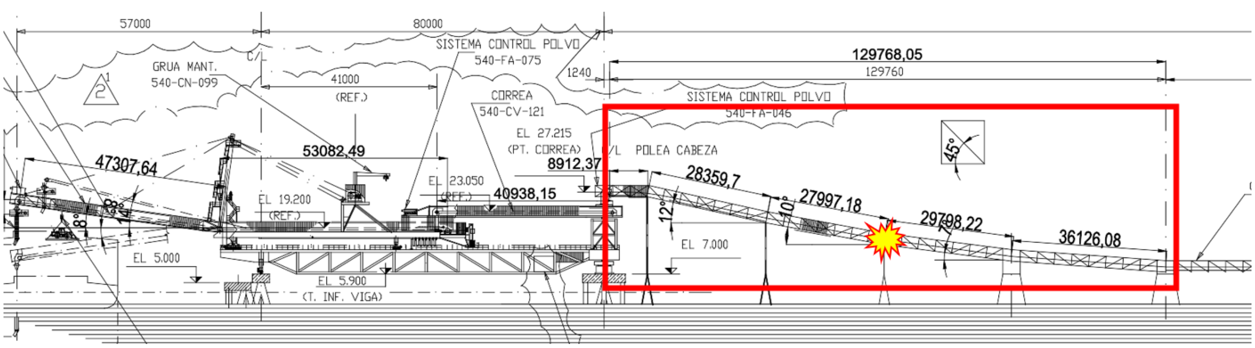

Figure 12: Fire Location

The geometry of the conveyor belt and the location is presented in the Figure 13, where is considered a belt with 1200mm width and 10mm thick. The enclosure is considered as a metal sheet with the properties specified in the Table 3. Inside of the passageway where the conveyor is located, there is no airflow while the equipment is stopped, while is considered that every ventilation and equipment working will halt in case a fire is detected in the conveyor belt.

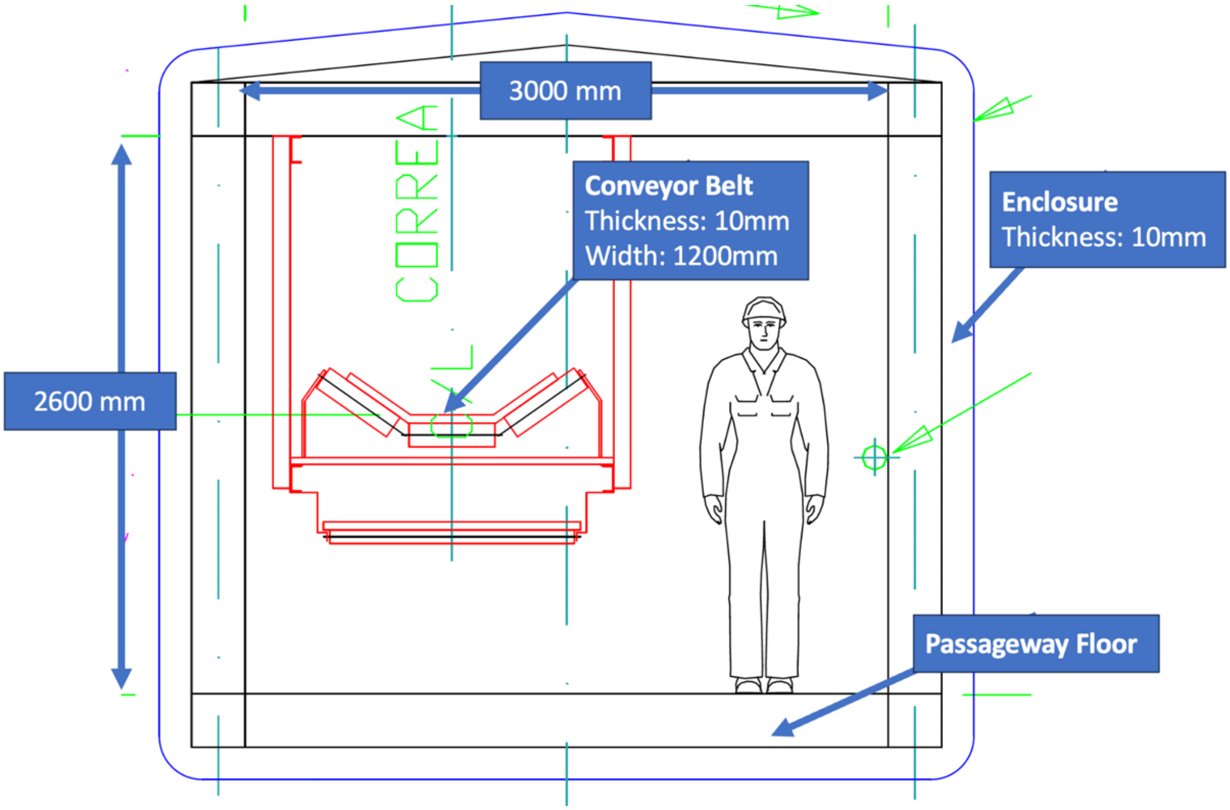

Figure 13: Conveyor Belt Geometry

Table 3: Enclosure material´s properties

Specific Heat	0.46	kJ/(kg°K)
Conductivity	45.8	W/(m°K)
Density	7850	kg/m3
Emissivity	0.95	Dimensionless
Thickness	0.01	Meters

According to the results obtained in the simulation of scenario 01 – conveyor belt fire, the measured temperature in the return belt reaches values close to 32°C at 7 seconds. After 15 seconds after the fire ignition, the temperature in the return belt reaches values close to 44°C (Figure 14).

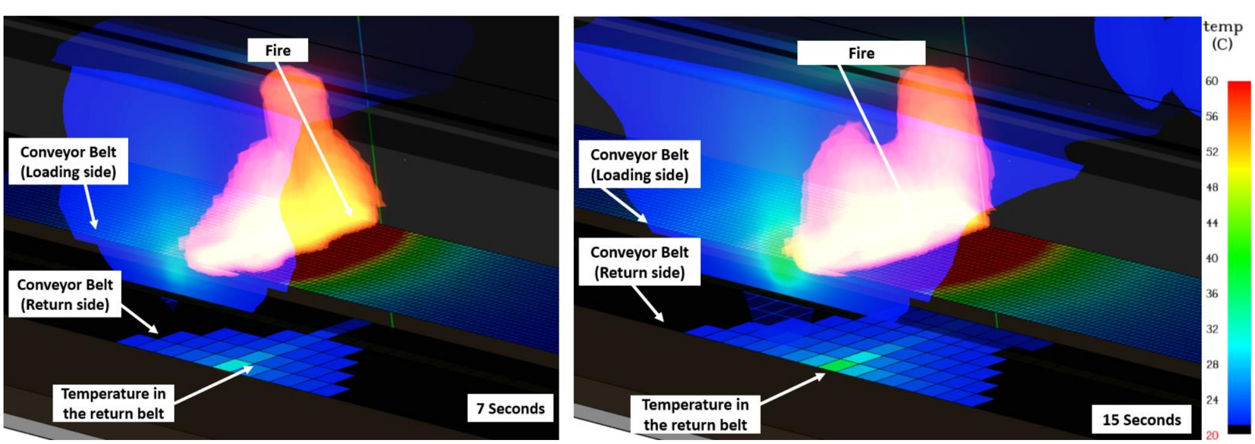

Figure 14: Temperatures in the conveyor belt due to the fire

The conveyor belt will be protected with an early fire detection system considered as Fibrolaser [6]. The before mentioned detection system operates in three different configurations, being able to trigger the alarm at temperature close to 40°C (Figure 15). Therefore, for the deluge systems or water mist systems operated by a detection system, the nozzles will operate after 15 seconds after the beginning of the ignition.

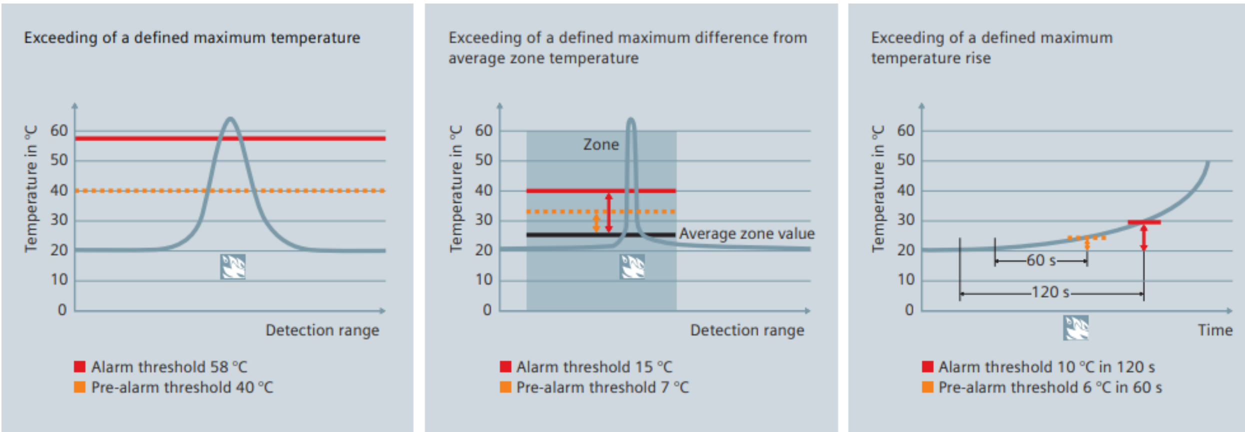

Figure 15: Fibrolaser System

<u>Fire Scenario 02 - Conveyor Belt Active Fire Protection</u>

<u>The current fire scenario considers the entire scenario described in the title “Fire Scenario 01 - Conveyor Belt Fire” and is complemented with the active fire protection systems considered in the title “Mesh and Cell Size</u>

For the initial grid resolution, the expression stated in the FDS User Guide has been considered. For simulations involving buoyant plumes, a measure of how well the flow field is resolved is given by the non-dimensional expression $\frac{D*}{\delta x}$, where D* is a characteristic fire diameter and δx is the nominal size of a mesh cell.

$$D^* = (\frac{Q}{\rho\ C\ T\ \sqrt{g}})^{\frac{2}{5}} \qquad \text{Equation 5}$$

Where $\dot{Q}$ is heat release rate of the fire is, ρ is the air density at ambient temperature, C correspond to the air specific heat, T is the ambient temperature and g is the acceleration due to gravity. In a sensitivity analysis (Hill et al., 2007), sponsored by the U.S. Nuclear Regulatory Commission, the D * / Δx value ranges between 4 and 16.

As a cell size criterion, the following relationship of numerical intervals will be used, where 4 will correspond to a poor resolution without affecting the values of the results and 16 will correspond to the greatest resolution without demanding a high cost of computational resources.

$$4 < \frac{D^*}{\delta x} < 16 \qquad \text{Equation 6}$$

Thus, by applying the before mentioned criteria and considering the values shown in the Table 4 it is possible to obtain the flow resolution quality indicator values for the combustion zone, and the plume zone of the hot gases produced by the fire in the conveyor belt.

Table 4: Parameters considered.

Ambient Temperature	1.2	kg/m3
Cp Ambient Air	1	kJ/kg °K
Ambient Temperature	293	°K
Gravity Acceleration	9.81	m/s2

The mesh geometry will be built considering cubic cells with a symmetrical configuration. The entire computational domain will be divided into different meshes with different cell sizes, allowing to cover the computational domain without overusing cells.

The Figure 17 contains the meshing technique, where the conveyor belt zone contains the smallest cell in the domain and then the fire plume contains cells with a middle size. The biggest cell size is used in the lower part of the domain, where the fresh air inlet for the fire is located.

The sensitivity analysis for the cell size shown in the Figure 17 and according to the to the Equation 5 and Equation 6 is indicated in the Table 5 and Table 6, where and indicator of a great flow resolution is shown.

The 2 MW used as a prior HRR to assess the sensitivity analysis it has been developed by previous research [], where it is possible to find that the early stage of the fire in a similar conveyor belt develop a HRR of 2MW (Figure 16).

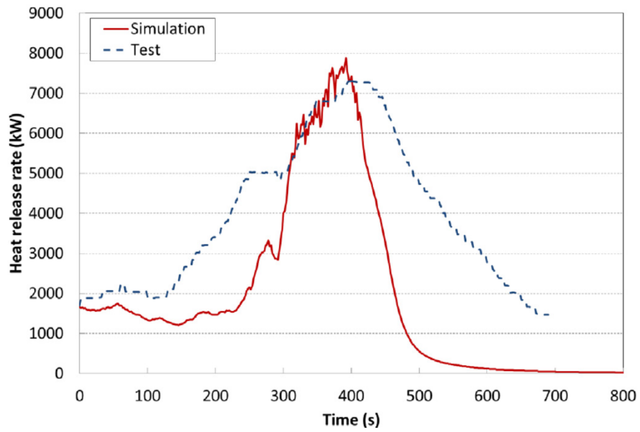

Figure 16: HRR Simulated and tested in a similar conveyor belt.

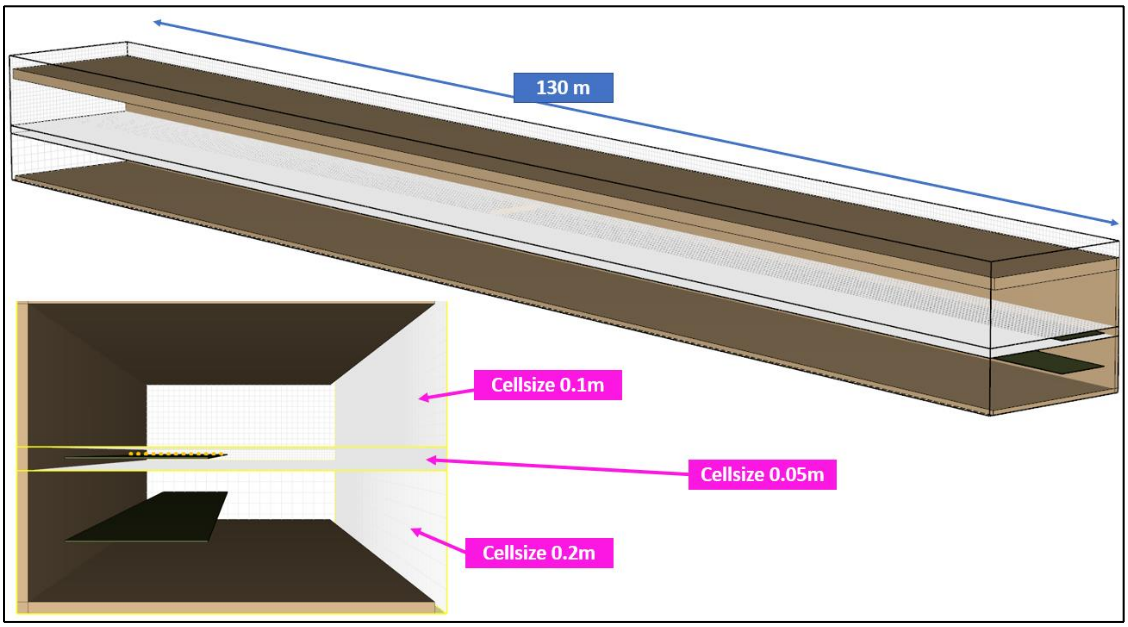

Figure 17: Meshing technique

Table 5: Cellsize Combustion Zone

Scenario	HRR		D*	Cellsize (m)	D*/Cellsize
Scenario 01	2000	kW	0.8041	0.05	16
Scenario 02-05-A	2000	kW	0.8041	0.05	16
Scenario 02-05-B	2000	kW	0.8041	0.05	16
Scenario 02-05-C	2000	kW	0.8041	0.05	16
Scenario 02-05-D	2000	kW	0.8041	0.05	16

Table 6: Cellsize Plume Zone

Scenario	HRR		D*	Cellsize (m)	D*/Cellsize
Scenario 01	2000	kW	0.8041	0.1	8
Scenario 02-05-A	2000	kW	0.8041	0.1	8
Scenario 02-05-B	2000	kW	0.8041	0.1	8
Scenario 02-05-C	2000	kW	0.8041	0.1	8
Scenario 02-05-D	2000	kW	0.8041	0.1	8

TRIAL DESIGNS" of the current study.

- **The fire scenario 02, sub scenario 05-A** contemplates the fire protection of the conveyor belt with sprinklers quick response, K=8.0 (115), operating pressure = 15 PSI and a temperature rating of 165ºF (74ºC).

- **The fire scenario 02, sub scenario 05-B** contemplates the fire protection of the conveyor belt with sprinklers quick response, K=5.6 (80.6), operating pressure = 15 PSI and a temperature rating of 165ºF (74ºC).

- **The fire scenario 02, sub scenario 05-C** contemplates the fire protection of the conveyor belt with sprinklers standard response, K=5.6 (80.6), operating pressure = 15 PSI and a temperature rating of 165ºF (74ºC).

- **The fire scenario 02, sub scenario 05-D** contemplates the fire protection of the conveyor belt with open water mist spray nozzles, K=2.04 lpm/bar1/2, operating pressure = 100 Bar.

Fire Scenario 02 – 05-A, 05-B, 05-C

Sprinklers System – Number of Droplets

According to test and analysis assessed by the WPI [7], it is concluded that run FDS with more particles than the default (5000), will not improve the prediction of the water bucket test for a sprinkler K=5.6. Therefore, it is considered 5000 droplets.

Sprinklers System – Droplets Size Estimation

According to David Sheppard´s investigation [8], several sprinkles with similar features than the sprinklers considered in the current study has been tested, presenting droplets sizes Dv50 between 700 to 1000 μm.

There is a mathematical correlation to estimate the sprinkler droplet size [9] and is described following.

$$\frac{Dv_{50}}{D_n} = CW_e{}^{-1/3} \qquad \text{Equation 1}$$

Where Dv_{50} correspond to the mean value of droplets discharged by the sprinkler, D_n correspond to the sprinkler diameter, C is a constant sprinkler dependent with values between 1.74 - 3.21, and W_e correspond to the Weber number, which one is calculated as following.

$$\frac{We = \rho_l * U_j^2 * D_n}{\sigma} \qquad \text{Equation 2}$$

Where ρ_l corresponds to the density of water, σ corresponds to the surface tension, U corresponds to the velocity of the discharged water by the sprinkler. Therefore, the droplet size (Dv50) will be estimated for the sprinklers to be used in the computer simulations.

Sprinklers System – Droplet Initial Velocity

The droplet initial velocity can be computed based on mean flow velocity, which depends on the injection pressure and the discharge coefficient, according to the following equation.

$$V_0 = C * \sqrt{\frac{\Delta P}{\rho}} \qquad \text{Equation 3}$$

Where V_0 is the initial velocity in m/s, ρ is the density of water in kg/m3 and ΔP is the relative pressure at the nozzle in Pascals. The parameter C is a factor used to take into account friction losses in the nozzle. It has not been determined experimentally and typically, the value of C varies between 0.5 and 1, which corresponds to initial velocity values between 22 and 45 m/s [10].

Sprinklers System – Discharge Coefficient

The discharge coefficient (K) relates the physical and geometrical features of the nozzle and the operation pressure of the device. Besides, the K factor considers the behavior of the vena contracta of the flow and the flow that is discharging through the nozzle. The K factor can be computed according to the following equation.

$$K = \frac{Q}{\sqrt{P}} \qquad \text{Equation 4}$$

Where the flow Q is measured in liter per minute, the relative pressure P at the nozzle is in Bar or MPa and the discharge coefficient K is in L/m/bar1/2.

<u>Fire Scenario 02 – 05-D</u>

Water Mist System – Number of Droplets

The default number of particles per second used in sprinkler modeling in the FDS package corresponds to 5000. Most research and studies in simulations were achieved with 1.0, 1.5 and 2, 0 x 10^5 particles per second for watermist discharge nozzles [11].

Counting small particles caused numerical instability when the particles hit the hot surface and the higher flows aggravated the phenomenon. Therefore, the number of particles that has been chosen to simulate the watermist nozzle will correspond to 100,000, according to the results obtained in sensitivity analysis [12].

Water Mist System – Droplets Size

There are different quantities to characterize the size of the droplets in the sprinkler discharge. In fact, sprinkler discharge consists of millions of droplets with a certain size distribution. One quantity is the volume median diameter Dv 50, which is the diameter defined such that half the volume of the water is contained in droplets with a diameter less than Dv 50 (and therefore half the water is contained in droplets with a diameter greater than Dv 50).

According to what is indicated by the average manufacturers of water mist systems, a droplet size of 120 um is considered [13].

Water Mist System – Technical Nozzle Specification

Revisión: Review: 01	**FICHA TECNICA / DATA SHEET**	Codigo: Code:	
Fecha: Date: 29-01-13	**DIFUSOR ABIERTO APLI. LOCAL EMM-540856**	Nº F.Técnica/Fichero: Data Sheet No./File:	fa008cs1.dwg
Hoja: Sheet: 1/1	**OPEN NOZZLE LOCAL APPLICATION EMM-540856**	Sistema de Extinción: Extinguish System:	RG W-FOG Agua Nebulizada

Descripción
Description

Difusor abierto de agua nebulizada para riesgos protegidos por aplicación local. Descargan el agente extintor dentro de la zona protegida asegurandose una correcta distribución del flujo. El cabezal esta formado por dos cuerpos que facilitan la instalación y el mantenimiento. Cada difusor está compuesto por un nº determinado de microdifusores en función de las características de la aplicación.

Water Mist open nozzle for local application protected risks. They discharge extinguishing agent into protected zone, assuring the correct flow distribution. Head is compounded of two bodies that makes easier the installation and maintenace operations. Each nozzle is compounded of a determinated number of micronozzles, according to the application characteristics.

Esquema
Scheme

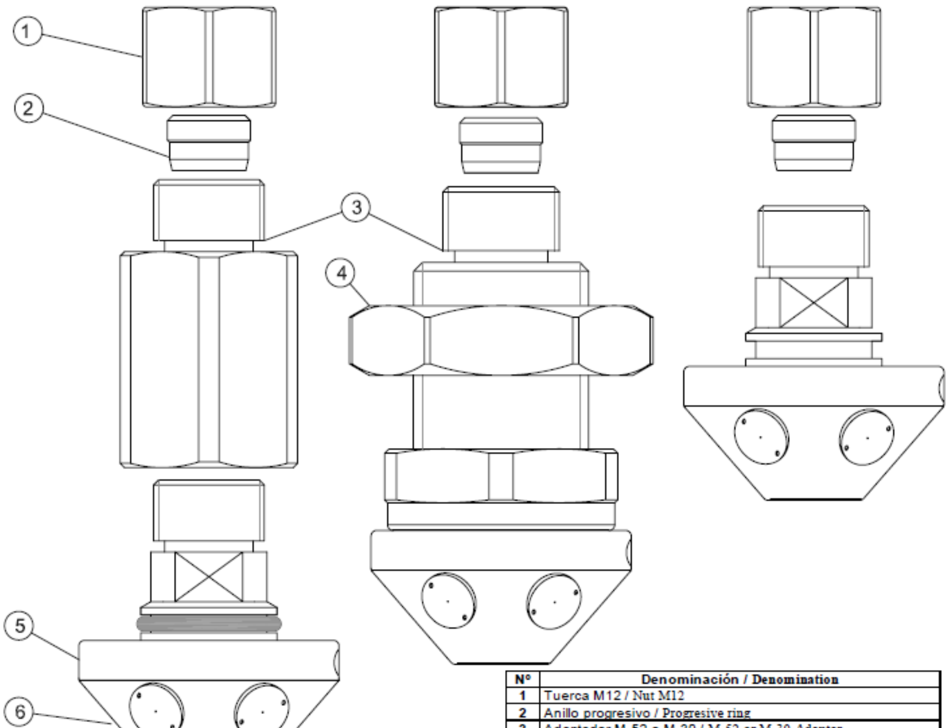

Nº	Denominación / Denomination
1	Tuerca M12 / Nut M12
2	Anillo progresivo / Progresive ring
3	Adaptador M-52 o M-30 / M-52 or M-30 Adaptor
4	Tuerca M-30 / M-30 Nut
5	Difusor EMM-540856 / Nozzle EMM-540856
6	Microdifusor / Micronozzle

Características técnicas
Characteristics technical

Medio operativo / Operating medium	Agua nebulizada alta presión / High pressure water mist
Material del difusor / Nozzle material	Acero INOX / INOX Steel
Material del microdifusor / Micronozzle material	Acero INOX / INOX Steel
Material del adaptador M-52 / M-52 Adaptor material	Acero INOX / INOX Steel
Unión a tubería / Pipe union	Mediante anillo progresivo en bicono. Tubería de 12x1.5mm / With progresive ring bi-cone. Pipe 12x1.5mm
Máxima presión de trabajo / Max. working pressure	200 bar
Presión de prueba / Test pressure	620 bar
Temperatura de trabajo / Working temperature	-20º C to +600º C
Temperatura de ensayo de resistencia a la presión y al calor / Heat and pressure proof temperature	600º C
Factor K / K Factor	2.04 l.p.m. / bar $^{1/2}$
Instalación / Instalation	Horizontal o pendiente / Horizontal or slope
Aplicación / Aplication	Aplicación local / Local aplication

Aviso
Warning

Este tipo de difusores, están fabricados y aprobados para ser usados en instalaciones fijas de proteccion contra incendios con Agua Nebulizada a alta presión. Estos productos no están diseñados para otro uso o propósito. Si el usuario del producto tiene alguna duda respecto a la aplicación o fin del producto, debe llamar al teléfono +34 947 28 11 08. Todo uso o aplicación no aprobado y / o cualquier no-aprobada modificación del producto o su funcionamiento puede provocar serios accidentes y / o daños personales. **RG Systems S.L.** no es responsable de ningún no-aprobado uso o aplicación.

This type of nozzles, are manufactured and approved to be used in fixed protected against fire installations with high pressure Water Mist. These products are not designed for other use or purpose. If product user has any doubt regarding the application or product use, please contact +34 947 28 11 08. Every not approved use or application or / and any other not approved modification of the product or its function may cause serious accidents or / and personal damages. **RG Systems S.L.** is not responsable for any non-approved use of the application.

IMPORTANTE: RG Systems S.L., se reserva el derecho a modificar sin previo aviso cualquier dato o especificación reflejada en este documento con el propósito de realizar cambios o mejoras en los productos presentados.
IMPORTANT: RG Systems S.L. reserves the right to change or modify without previous notice any data or specification due to changes or modification in order to improve the products presented.

Dibujado: Draw by:	C. Francés	Firma / Signed by	Sustituye a: Substitution to:	06-08-07	RG SYSTEMS Pol. Ind. Villalonquejar C/Merindad de Montija Nº6 (09001) Burgos - España Tel.- 947281108 Fax.-947281112
Comprobado: Check by:	J.I.Melgosa		Sustituido por: Sustituyed by:		

Mesh and Cell Size

For the initial grid resolution, the expression stated in the FDS User Guide has been considered. For simulations involving buoyant plumes, a measure of how well the flow field is resolved is given by the non-dimensional expression $\frac{D*}{\delta x}$, where D* is a characteristic fire diameter and δx is the nominal size of a mesh cell.

$$D^* = (\frac{Q}{\rho\ C\ T\ \sqrt{g}})^{\frac{2}{5}} \qquad \text{Equation 5}$$

Where $\dot{Q}$ is heat release rate of the fire is, ρ is the air density at ambient temperature, C correspond to the air specific heat, T is the ambient temperature and g is the acceleration due to gravity. In a sensitivity analysis (Hill et al., 2007), sponsored by the U.S. Nuclear Regulatory Commission, the D * / Δx value ranges between 4 and 16.

As a cell size criterion, the following relationship of numerical intervals will be used, where 4 will correspond to a poor resolution without affecting the values of the results and 16 will correspond to the greatest resolution without demanding a high cost of computational resources.

$$4 < \frac{D^*}{\delta x} < 16 \qquad \text{Equation 6}$$

Thus, by applying the before mentioned criteria and considering the values shown in the Table 4 it is possible to obtain the flow resolution quality indicator values for the combustion zone, and the plume zone of the hot gases produced by the fire in the conveyor belt.

Table 4: Parameters considered.

Ambient Temperature	1.2	kg/m3
Cp Ambient Air	1	kJ/kg °K
Ambient Temperature	293	°K
Gravity Acceleration	9.81	m/s2

The mesh geometry will be built considering cubic cells with a symmetrical configuration. The entire computational domain will be divided into different meshes with different cell sizes, allowing to cover the computational domain without overusing cells.

The Figure 17 contains the meshing technique, where the conveyor belt zone contains the smallest cell in the domain and then the fire plume contains cells with a middle size. The biggest cell size is used in the lower part of the domain, where the fresh air inlet for the fire is located.

The sensitivity analysis for the cell size shown in the Figure 17 and according to the to the Equation 5 and Equation 6 is indicated in the Table 5 and Table 6, where and indicator of a great flow resolution is shown.

The 2 MW used as a prior HRR to assess the sensitivity analysis it has been developed by previous research [14], where it is possible to find that the early stage of the fire in a similar conveyor belt develop a HRR of 2MW (Figure 16).

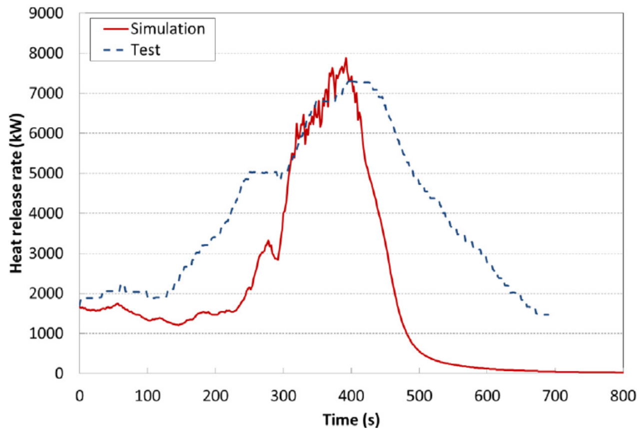

Figure 16: HRR Simulated and tested in a similar conveyor belt.

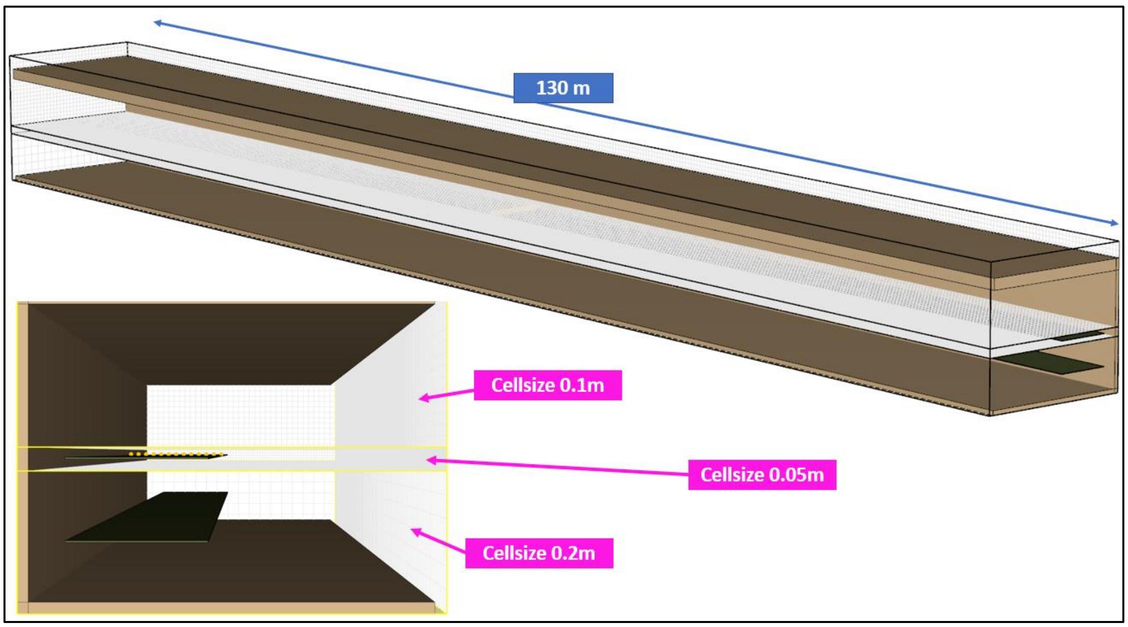

Figure 17: Meshing technique

Table 5: Cellsize Combustion Zone

Scenario	HRR		D*	Cellsize (m)	D*/Cellsize
Scenario 01	2000	kW	0.8041	0.05	16
Scenario 02-05-A	2000	kW	0.8041	0.05	16
Scenario 02-05-B	2000	kW	0.8041	0.05	16
Scenario 02-05-C	2000	kW	0.8041	0.05	16
Scenario 02-05-D	2000	kW	0.8041	0.05	16

Table 6: Cellsize Plume Zone

Scenario	HRR		D*	Cellsize (m)	D*/Cellsize
Scenario 01	2000	kW	0.8041	0.1	8
Scenario 02-05-A	2000	kW	0.8041	0.1	8
Scenario 02-05-B	2000	kW	0.8041	0.1	8
Scenario 02-05-C	2000	kW	0.8041	0.1	8
Scenario 02-05-D	2000	kW	0.8041	0.1	8

TRIAL DESIGNS

The following trial designs contemplate the fire protection strategy that is intended to fulfill the goals and objectives of the study. To be considered acceptable, the trials designs must achieve the performance criteria indicated earlier. The following described trial designs are grouped in the following categories,

- Ignition and spreading of fire, due to the methods are used to reduce the probability of ignition and/or reduce the heat release rate of a fire.

- Fire suppression, including automatic and/or manual fire protection systems.

The trial designs are evaluated in the fire scenario 01 described earlier in the current document.

Scenario 05-A

The current scenario presents the following considerations.

- Sprinklers that correspond to FM approved quick response with a K factor of 8.0 (115) and a temperature rating of 165ºF (74ºC).
- Operating pressure = 15 PSI.
- The RTI corresponds to 50 $m^{1/2}*s^{1/2}$ (quick response sprinkler).
- The separation distance between sprinklers corresponds to 3.5m.
- The installation distance from the roof of the passageway corresponds to 0.2m.
- According to the sprinkler´s manufacturer [15], the discharge pattern for the operating pressure (15 PSI) corresponds to an angle of 55°.

Table 7: Sprinkler´s parameters and droplet size for modelling

Density	1000	kg/m3
Superficial Tension	0.0728	N/m
Dn	20	mm
	0.02	mm
Sprinkler Area	0.00031415	m2
Sprinkler Flow	31	gpm
	1.953	l/s
	117.18	lpm
	0.001953	m3/s
Water flow speed	6.21	m/s
Weber Number	10618	
Dv50	0.0022748	m
	2.2748	mm
	2274.8	um

Scenario 05-B

The current scenario presents the following considerations.

- Sprinkler selected K factor = 5.6 (80.6) and temperature rating of 165ºF (74ºC).
- Operating pressure = 15 PSI.
- The RTI correspond to 50 $m^{1/2}*s^{1/2}$ (quick response sprinkler).
- The separation distance between sprinklers corresponds to 3.5m.

- The installation distance from the roof of the passageway corresponds to 0.2m.
- According to the sprinkler´s manufacturer [16], the discharge pattern for the operating pressure (15 PSI) corresponds to an angle of 56°.

Table 8: Sprinkler´s parameters and droplet size for modelling

Density	1000	kg/m3
Superficial Tension	0.0728	N/m
Dn	15	mm
	0.015	mm
Sprinkler Area	0.0001767	m2
Sprinkler Flow	21.7	gpm
	1.3671	l/s
	82.02	lpm
	0.0013671	m3/s
Water flow speed	7.736432	m/s
Weber Number	12332	
Dv50	0.00162312	m
	1.62312	mm
	1623.12	um

Scenario 05-C

The current scenario presents the following considerations.

- Sprinklers selected with a K factor of 5.6 (80.6) and a temperature rating of 165ºF (74ºC).
- Operating pressure = 15 PSI.
- The RTI correspond to 100 $m^{1/2}*s^{1/2}$ (standard response sprinkler).
- The separation distance between sprinklers corresponds to 3.5m.
- The installation distance from the roof of the passageway corresponds to 0.2m.
- According to the sprinkler´s manufacturer [17], the discharge pattern for the operating pressure (15 PSI) corresponds to an angle of 56°.

Table 9: Sprinkler´s parameters and droplet size for modelling

Density	1000	kg/m3
Superficial Tension	0.0728	N/m
Dn	15	mm
	0.015	mm
Sprinkler Area	0.0001767	m2
Sprinkler Flow	21.7	gpm
	1.3671	l/s
	82.02	lpm
	0.0013671	m3/s
Water flow speed	7.736432	m/s
Weber Number	12332	
Dv50	0.00162312	m
	1.62312	mm
	1623.12	um

Scenario 05-D

The current scenario presents the following considerations.

- The system considered corresponds to local application, machinery space.
- The nozzles would be completely stainless steel, with an M12 nut and connection to the pipe by a bi-cone ring.
- The maximum working pressure must be 200 Bar and the test pressure must be 600 Bar.
- The montage will be pendent at 0.2m under the roof.
- The discharge coefficient K=2.04 lpm/bar1/2.
- Maximum spacing according to the manufacturer corresponds to 4.7m, but they are considered installed spaced at 4m.
- Operating pressure corresponds to 100 Bar.
- It is considered 3 nozzles working after 15 seconds of fire started (See Fire Scenario 01 - Conveyor Belt Fire)

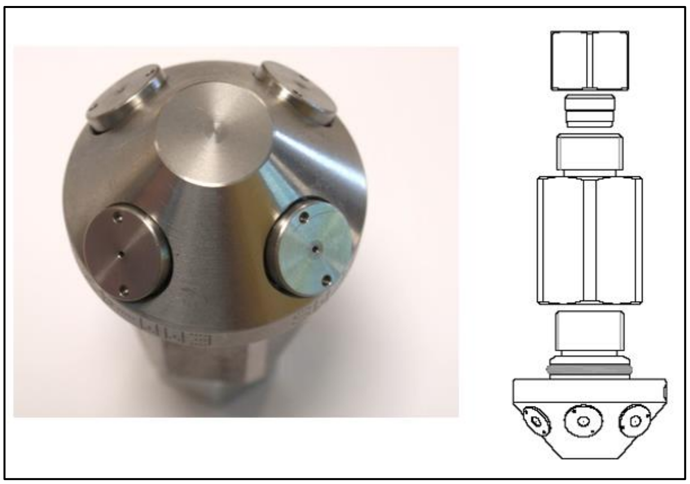

Figure 18: Nozzle Considered

EVALUATION OF TRIAL DESIGNS

Scenario 05-A

The Figure 19 contains the activation sequence of the trial design, where it is possible to observe that the first sprinkler operates at 16.4 seconds and the last of the five opened at 28.2 seconds from the beginning of the fire ignition (Figure 20).

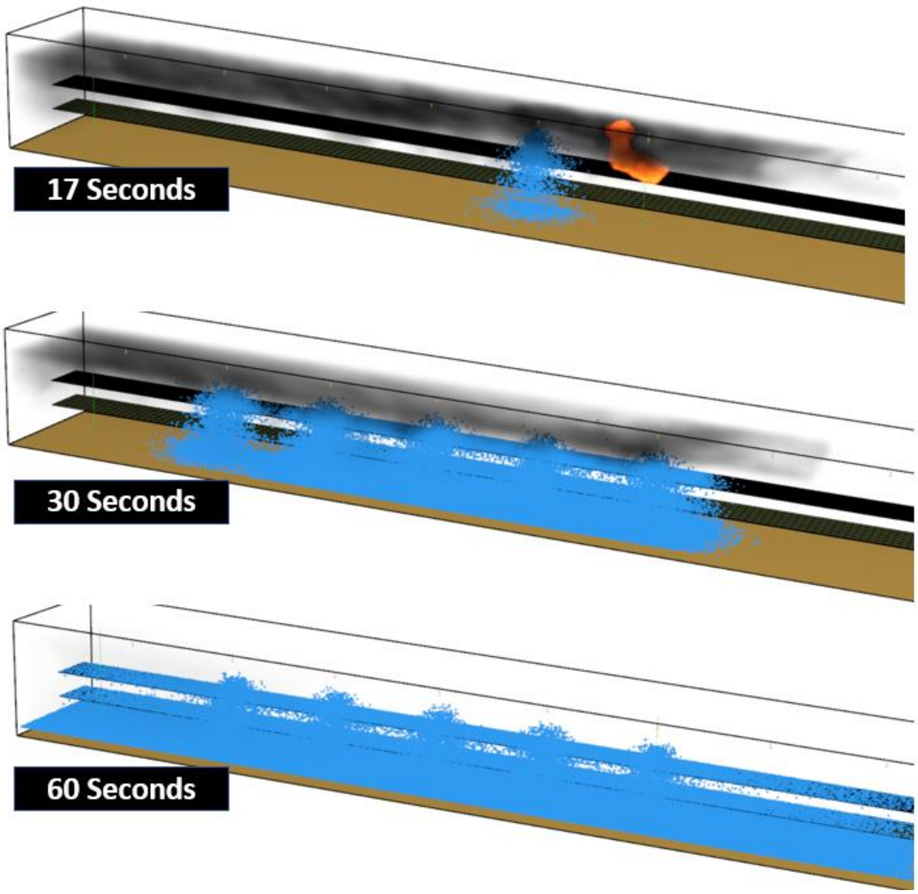

Figure 19: Activation Sequence

DEVICE Activation Times

7	SPRK-12	No Activation
8	SPRK-11	28.2 s
9	SPRK-08	23.3 s
10	SPRK-07	19.4 s
11	SPRK-06	16.4 s
12	SPRK-05	24.0 s
13	SPRK-04	No Activation
14	SPRK-03	No Activation
15	SPRK-02	No Activation
16	SPRK-01	No Activation
17	SPRK-09	No Activation
18	SPRK-10	No Activation

Figure 20: Activation Time

In the Figure 21 it is shown the HRR development, where it is demonstrated that after 30 seconds of the ignition, the sprinklers system is capable of control and extinguish the fire, reducing the HRR to nearly 0. The Table 10 contains the summary results regarding to the sprinklers operated and the total flow discharged.

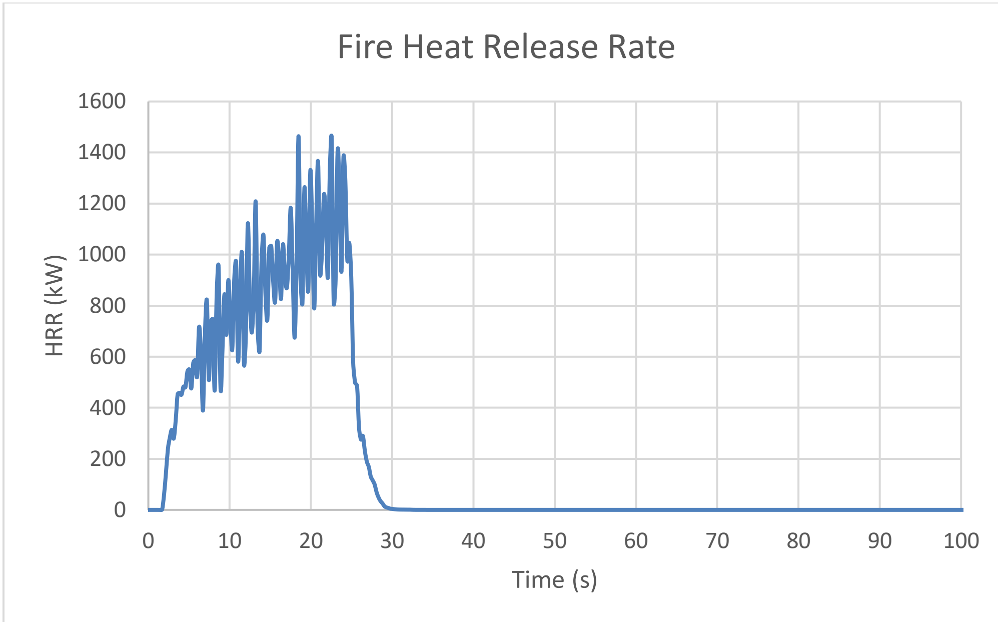

Figure 21: Heat Release Rate Evolution

Table 10: Summary results

Opened Sprinklers	5	Un
Total Flow	155	gpm
	586	lpm
Average Activation Time	22.3	sec

Scenario 05-B

The Figure 23 contains the activation sequence of the trial design, where it is possible to observe that the first sprinkler operates at 16.4 seconds and the last of the four opened at 23.4 seconds from the beginning of the fire ignition (Figure 22).

```
DEVICE Activation Times

 8   SPRK-12                                        No Activation
 9   SPRK-11                                        No Activation
10   SPRK-08                                            23.4 s
11   SPRK-07                                            19.5 s
12   SPRK-06                                            16.4 s
13   SPRK-05                                            23.2 s
14   SPRK-04                                        No Activation
15   SPRK-03                                        No Activation
16   SPRK-02                                        No Activation
17   SPRK-01                                        No Activation
18   SPRK-09                                        No Activation
19   SPRK-10                                        No Activation
```
Figure 22: Activation Time

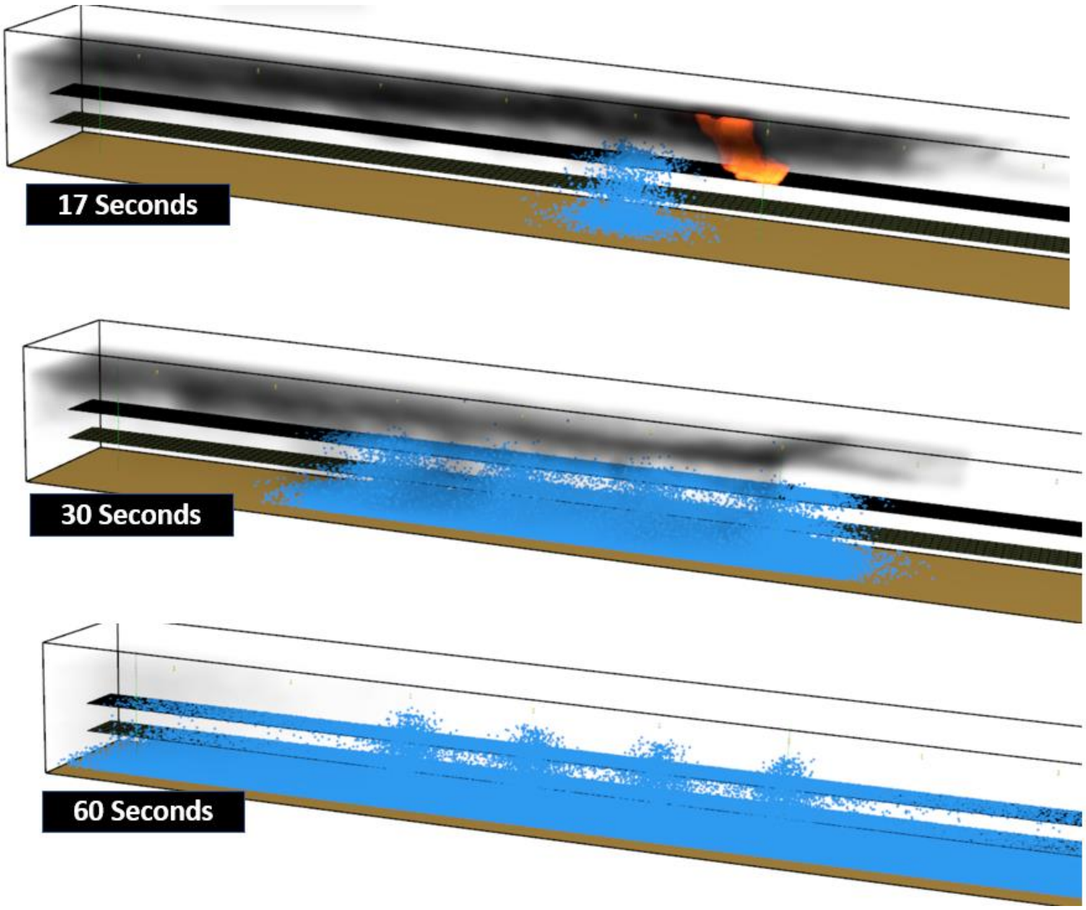

Figure 23: Activation Sequence

In the Figure 24 it is shown the HRR development, where it is demonstrated that after 30 seconds of the ignition, the sprinklers system is capable of control and extinguish the fire, reducing the HRR to nearly 0. The Table 11 contains the summary results regarding to the sprinklers operated and the total flow discharged.

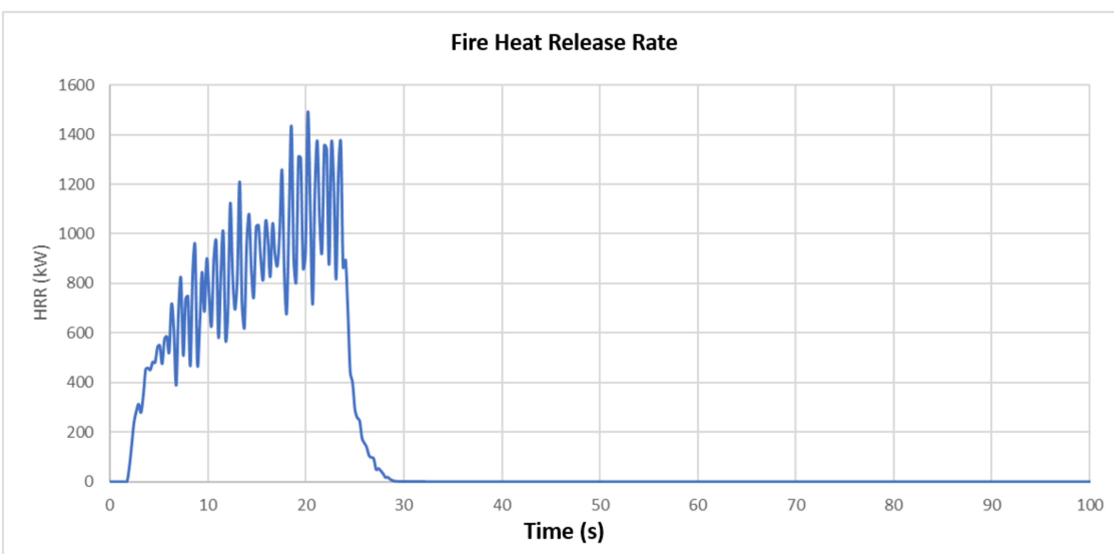

Figure 24: Heat Release Rate Evolution

Table 11: Summary results

Opened Sprinklers	4	Un
Total Flow	86.8	gpm
	328	lpm
Average Activation Time	20.6	sec

Scenario 05-C

The Figure 25 contains the activation sequence of the trial design, where it is possible to observe that the first sprinkler operates at 24.4 seconds and the last of the three opened at 27.8 seconds from the beginning of the fire ignition (Figure 26).

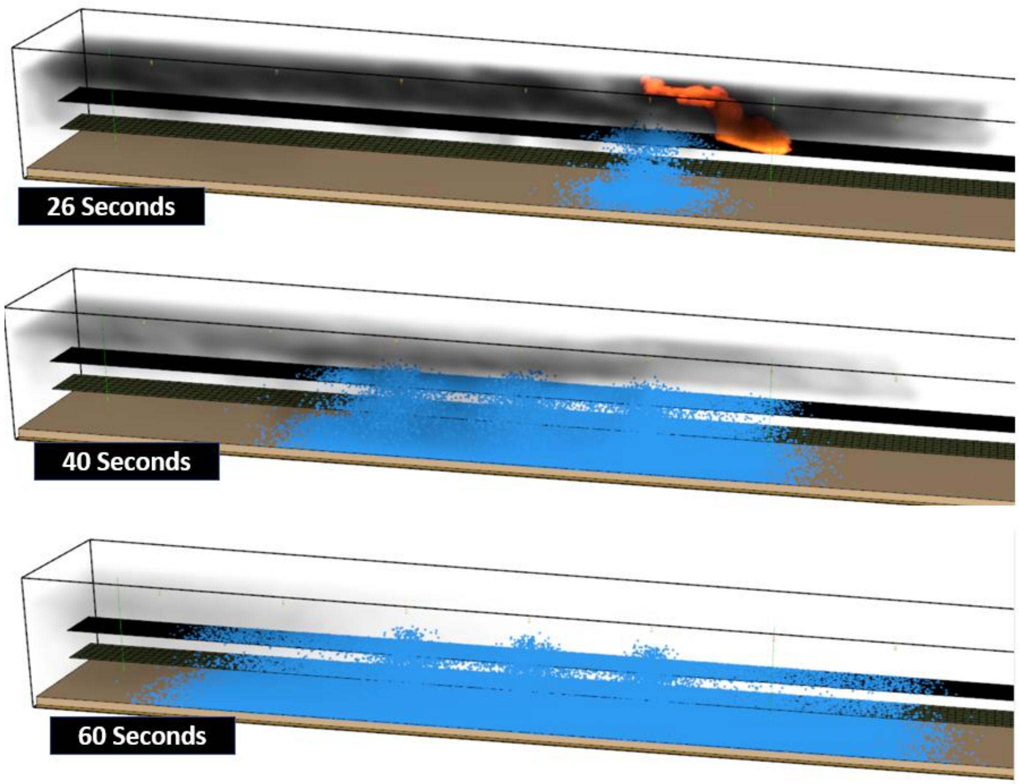

Figure 25: Activation Sequence

```
DEVICE Activation Times

  7  SPRK-12                                        No Activation
  8  SPRK-11                                        No Activation
  9  SPRK-08                                             32.7 s
 10  SPRK-07                                             27.8 s
 11  SPRK-06                                             24.4 s
 12  SPRK-05                                        No Activation
 13  SPRK-04                                        No Activation
 14  SPRK-03                                        No Activation
 15  SPRK-02                                        No Activation
 16  SPRK-01                                        No Activation
 17  SPRK-09                                        No Activation
 18  SPRK-10                                        No Activation
```

Figure 26: Activation Time

In the Figure 27 it is shown the HRR development, where it is demonstrated that after 38 seconds of the ignition, the sprinklers system is capable of control and extinguish the fire, reducing the HRR to nearly 0. The Table 12 contains the summary results regarding to the sprinklers operated and the total flow discharged.

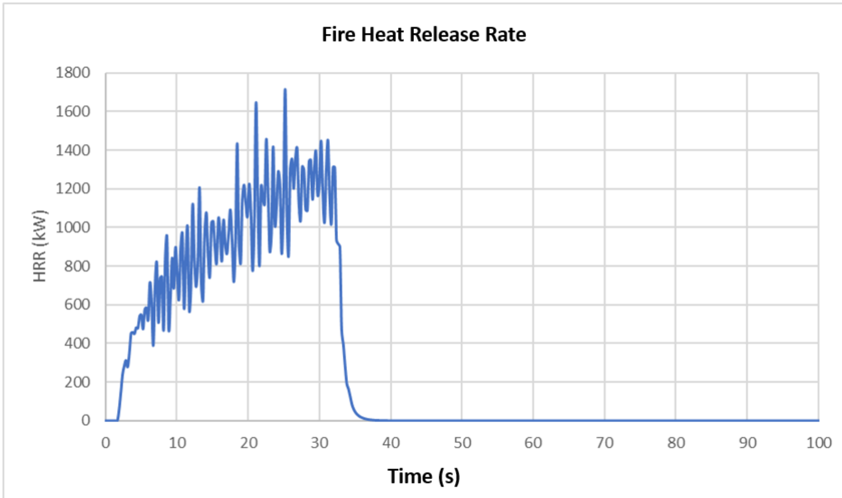

Figure 27: Heat Release Rate Evolution

Table 12: Summary results

Opened Sprinklers	3	Un
Total Flow	65.1	gpm
	246	lpm
Average Activation Time	28.3	seg

<u>Scenario 05-D</u>

The Figure 28 contains the activation sequence of the trial design, where it is possible to observe that the due to the nature of the configured system (deluge system) and the activation of the detection systems, 3 nozzles are activated and discharging water (Figure 29).

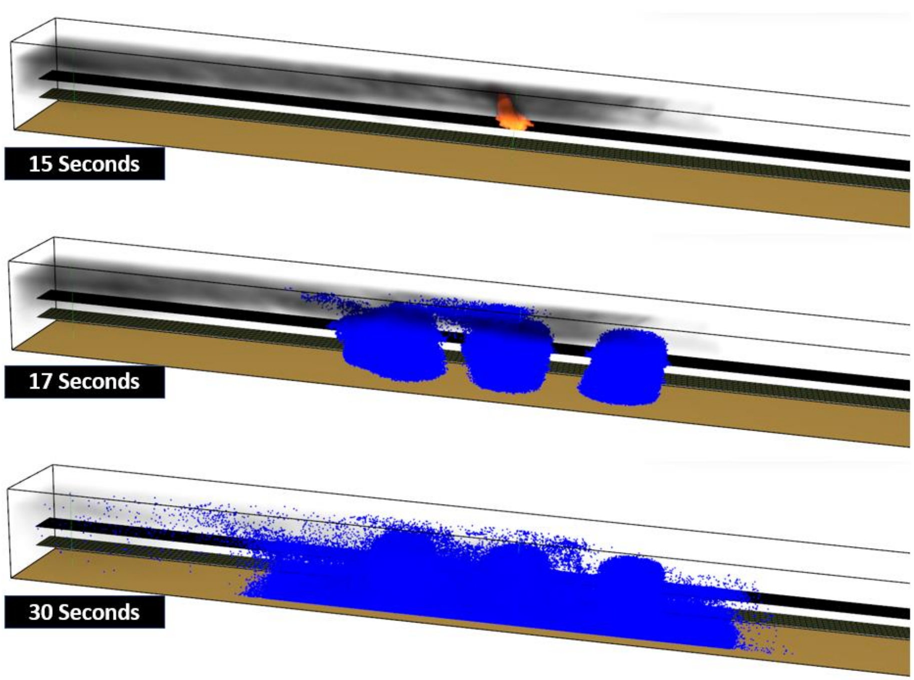

Figure 28: Activation Sequence

```
DEVICE Activation Times

  7  SPRK-06                                                      15.0 s
  8  SPRK-05                                                      15.0 s
  9  SPRK-04                                                      15.0 s
```

Figure 29: Activation Time

In the Figure 30 it is shown the HRR development, where it is demonstrated that after 18 seconds of the ignition, the sprinklers system is capable of control and extinguish the fire, reducing the HRR to nearly 0. The Table 13 contains the summary results regarding to the sprinklers operated and the total flow discharged.

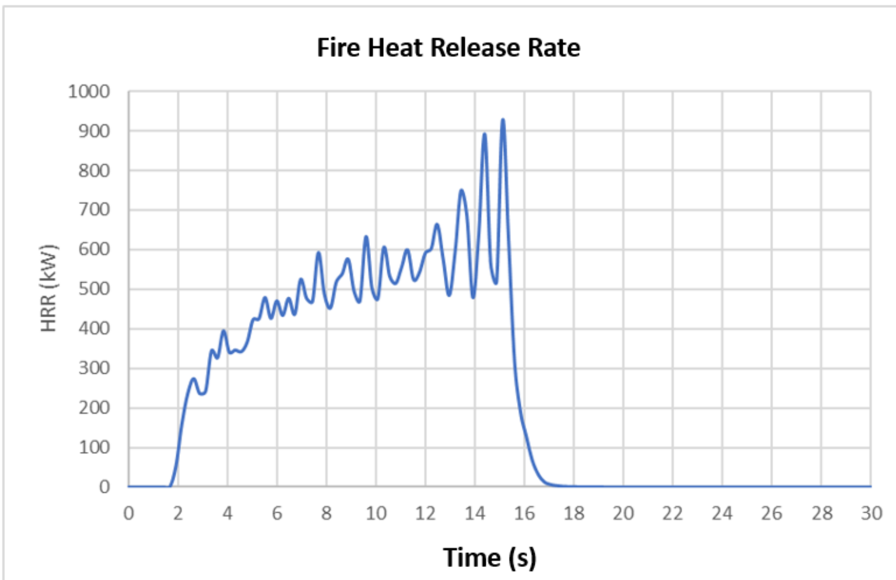

Figure 30: Heat Release Rate Evolution

Table 13: Summary results

Opened Sprinklers	3	Un
Total Flow	16.2	gpm
	61.2	lpm
Average Activation Time	15	Seg

RESULTS AND DISCUSSION

The heat release rate developed by the fire in each of the trial design is presented in the Figure 31. It is demonstrated that the water mist system controls and extinguish the fire in the shortest time compared with the sprinkler systems.

Besides, the average HRR developed in the sprinkler´s trial design is similar (Table 14). On the other hand, the HRR developed in the trial design of watermist releases a considerably less amount of energy compared with the sprinkler systems.

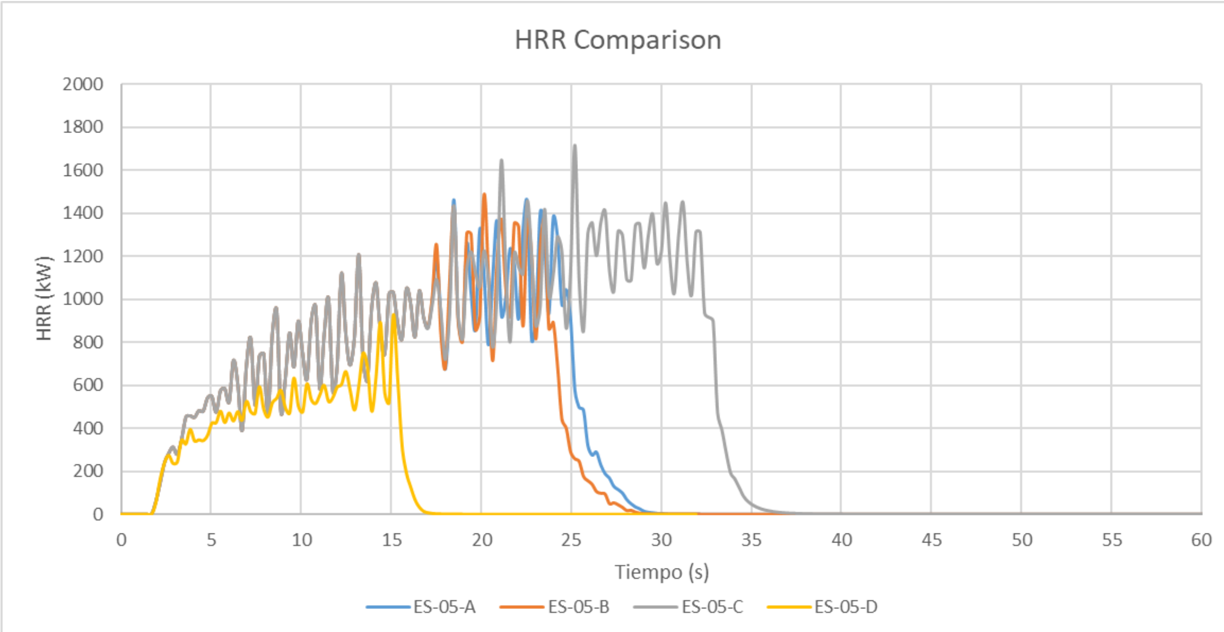

Figure 31: HRR Comparison

Table 14: HRR Average

	Trial Design			
	ES-05-A	ES-05-B	ES-05-C	ES-05-D
Average kW	584.67	565.77	607.03	338.18
	96.32%	93.20%	100%	55.71%

According to the information presented in the Figure 32, it is possible to indicate that the sprinklers system with the fastest activation time discharges the greatest amount of water.

On the other hand, the sprinkler system which activates the latest, delivers the least amount of water to control and extinguish the fire. The water mist system analyzed delivers the smallest amount of water to control and extinguish the fire.

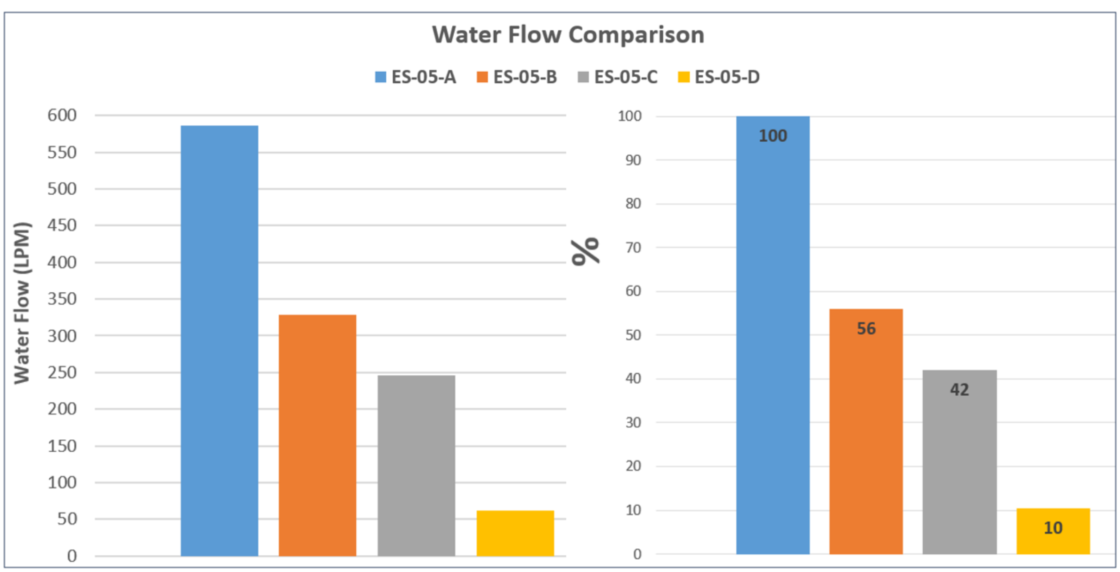

Figure 32: Water Flow Comparison

CONCLUSIONS

From the present study is possible to conclude that:

- The conventional and the modified sprinklers systems can control and extinguish a fire in the conveyor belt analyzed.

- It is possible to modify the sprinklers system indicated by FM Global. The modified sprinkler systems will permit to increase the HRR of the fire, but they will use less water than the FM Global design expects.

- The water mist system designed for the conveyor belt can control and extinguish the fire, using the configuration of local application and machinery space as design method.

- The water mist system designed for the conveyor will use just 10% of the water that FM-Global expects that controls and extinguish a fire in the conveyor belt.

- The less amount of water used in the water mist system allows the decrease the size of a drainage system in the conveyor belt, which will avoid the contamination of the sea water.

- Due to the water discharged will eventually contain cooper concentrated, a water collector tank must be placed in the conveyor belt system. Therefore, the reduced amount of water used in the water mist system allows to place a smaller water collector tank, compared with the sprinklers system.

- The HRR developed in each of the sprinklers system present similar average values. On the other hand, the HRR developed in the water mist system presents considerably lower values.

- The HRR developed in the water mist system is dependent on the activation time of the detection system.

- The detection time considered in the current study is conservative and fits the CFD estimation, but eventually could be higher.

REFERENCES

[1] Morgan J. Hurley. (2016). "SFPE Handbook of Fire Protection Engineering". Fifth Edition

[2] Design Fire Scenarios Involving Non-Fire Resistant Conveyor Belts -Numerical Study, Rickard Hansen, The University of Queensland

[3] Numerical and experimental study on flame spread over conveyor belts in a large-scale tunnel - Liming Yuan*, Richard J. Mainiero, James H. Rowland, Richard A. Thomas, Alex C. Smith

[4] SFPE the Handbook of Fire Protection Engineering – Ed 5.

[5] Numerical and experimental study on flame spread over conveyor belts in a large-scale tunnel - Liming Yuan*, Richard J. Mainiero, James H. Rowland, Richard A. Thomas, Alex C. Smith

[6] FibroLaser III – reliable fire protection for long and widespread systems – SIEMENS

[7] Computational modeling of fire sprinkler spray characteristics using the fire dynamics simulator, worcester polytechnic institute

[8] Spray Characteristics of Fire Sprinklers - David Thomas Sheppard, Northwestern University

[9] Spray Characteristics of Fire Sprinklers - David Thomas Sheppard, Northwestern University

[10] Numerical analysis of a water mist spray: The importance of various numerical and physical parameters, including the drag forcé, Yuanjun Liu, Tarek Beji, Martin Thielens, Zhi Tang, Zheng Fang, Bart Merci

[11] Lehtimaki, M. (2017). Simulation of Water Cooling in Fires. Aalto, Finland. School of Engineering Aalto University.

[12] CFD Study on the Interaction between Water Sprays and Longitudinal Ventilation in Tunnel Fires. Patricio Valdés – University of Ghent

[13] APPROXIMATE TRAVELLING DISTANCES OF WATER MIST DROPLETS IN TUNNELS - Richard Crosfield, Angelo Cavallo, Francesco Colella, Ricky Carvel, José L. Torero & Guillermo Rein BRE Centre for Fire Safety Engineering, University of Edinburgh, UK

[14] Numerical and experimental study on flame spread over conveyor belts in a large-scale tunnel - Liming Yuan*, Richard J. Mainiero, James H. Rowland, Richard A. Thomas, Alex C. Smith - Journal of Loss Prevention in the Process Industries

[15] VIKING Technical data - VK3521 quick response technical data pendent sprinkler (k8.0)

[16] VIKING Technical data - VK3021 quick response technical data pendent sprinkler (k5.6)

[17] VIKING Technical data – VK1021 quick response technical data pendent sprinkler (k5.6)